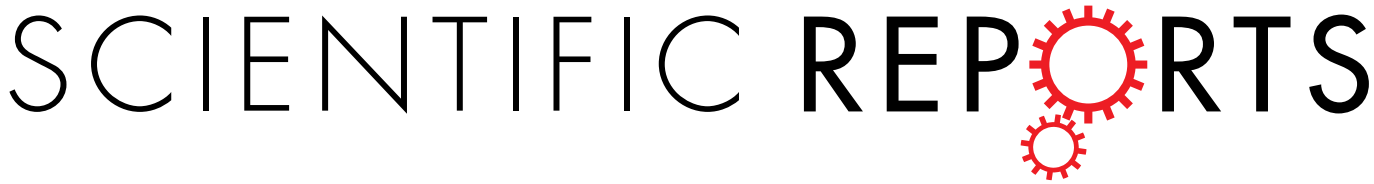

OPEN

Fast optical cooling of a nanomechanical cantilever by a dynamical Stark-shift gate

Received: 09 April 2015
Accepted: 02 September 2015
Published: 12 October 2015

Leilei Yan[1,2], Jian-Qi Zhang[1], Shuo Zhang[3] & Mang Feng[1]

The efficient cooling of nanomechanical resonators is essential to exploration of quantum properties of the macroscopic or mesoscopic systems. We propose such a laser-cooling scheme for a nanomechanical cantilever, which works even for the low-frequency mechanical mode and under weak cooling lasers. The cantilever is coupled by a diamond nitrogen-vacancy center under a strong magnetic field gradient and the cooling is assisted by a dynamical Stark-shift gate. Our scheme can effectively enhance the desired cooling efficiency by avoiding the off-resonant and undesired carrier transitions, and thereby cool the cantilever down to the vicinity of the vibrational ground state in a fast fashion.

Over the past years, nano-mechanical resonators (NRs) have attracted considerable attention both theoretically and experimentally and presented potential applications based on the quantum properties, for example, optomechanical induced transparency[1], photon blockade[2,3], optical Kerr effect[4], entanglement between microscopic objects[5,6], quantum state measurement[7,8], biological sensing detection[9,10] and hybrid coupling to cold atoms[11].

However, quantum properties regarding the NRs are always hidden by the thermal phonons involved. To suppress the thermal phonons, many schemes have been proposed so far to try to cool the NRs down to the vicinity of their vibrational ground states, such as the sideband cooling[12,13], the backaction sideband cooling[14–19], the hot-thermal-light-assisted cooling[20], the time-dependent control cooling[21,22], the quadratic-coupling-based cooling[23], the measurement cooling[24] and the electromagnetically induced transparency (EIT) cooling[25–29].

The EIT cooling works based on quantum interference, which enhances the first-order red-sideband transition for cooling, but eliminates the carrier transition and suppresses the first-order blue-sideband transition for heating[25–29]. In particular, it works efficiently even in the non-resolved sideband regime in the laboratory representation, i.e., with a large spontaneous emission rate. The EIT cooling was first proposed and experimentally implemented in the trapped-ion system[30,31], and then extended to other systems, including the quantum dot[25,27,28], the superconducting flux qubit[26] and the diamond nitrogen-vacancy (NV) center[29]. However, for the Rabi frequency comparable to the vibrational frequency of the NR, the prerequisite of the fast cooling, the existing cooling scheme could not work efficiently[29]. Therefore, developing an alternative scheme available for the NR cooling, which is faster and more efficient than the EIT cooling, is highly desirable[32]. On the other hand, a NV center coupled to a nanomechanical cantilever can be used to cool the cantilever vibration down to a quantum regime[29,33], where the coupling is from a magnetic field gradient (MFG). The extension of such a coupling is applicable to future scalable quantum information processor[33,34]. To this end, achievement of high-quality NRs and cooling low-frequency NRs are highly expected, but experimentally demanding.

[1]State Key Laboratory of Magnetic Resonance and Atomic and Molecular Physics, Wuhan Institute of Physics and Mathematics, Chinese Academy of Sciences, Wuhan, 430071, China. [2]University of the Chinese Academy of Sciences, Beijing 100049, China. [3]Zhengzhou Information Science and Technology Institute, Zhengzhou, 450004, China. Correspondence and requests for materials should be addressed to J.-Q.Z. (email: changjianqi@gmail.com) or M.F. (email: mangfeng@wipm.ac.cn)

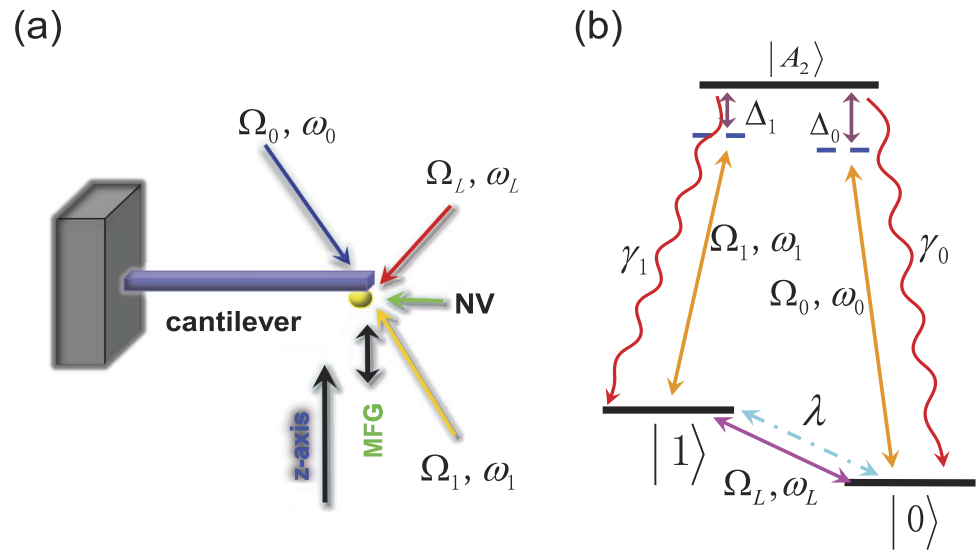

Figure 1. (**a**) Schematic illustration of our cooling scheme using a dynamic Stark-shift gate, where the nanomechanical cantilever is attached by a NV center under irradiation of lasers and an effective classical field. (**b**) The three levels form our major part of the cooling, where the irradiation of the two lasers satisfies the two-photon resonance with $\Delta_0 = \Delta_1$ and the effective classical field is in resonance with the transition between the two ground states, i.e., $\omega_L = \omega_0 - \omega_1$. The cantilever vibration is coupled to the NV center by a strong MFG. γ_0 (γ_1) is the decay from the excited state $|A_2\rangle$ to the ground state $|0\rangle$ ($|1\rangle$).

The present work focuses on the ground-state cooling of a NR with the assistance from a Stark-shift gate in the non-resolved sideband regime in the laboratory representation. Such a cooling scheme can cool a low-frequency ($\leq$1 MHz) NR more efficiently than the conventional sideband cooling due to elimination of the involved carrier transitions which contribute for heating, as confirmed in[32] for cooling the trapped ion. However, compared to the trapped ion, the NR (i.e., the cantilever) under consideration is of a much bigger mass, which decreases the mechanical effect of light on the NV-cantilever to nearly zero. To generate a strong enough coupling between the NV center and the cantilever, we introduce a strong MFG, as discussed in[29]. Moreover, since the cantilever is more sensitive to the environmental noise than the trapped ion, we have to seriously consider the influence from the non-zero temperature thermal noise of the environment in our calculation.

The key point in the present work is the introduction of an effective classical field to couple the sublevels of the electronic ground state of the NV center, which creates a dynamical Stark shift under the strong MFG and accelerates the cooling of the cantilever by suppressing the undesired transitions. We show the possibility to cool the cantilever with the same cooling rate as in the trapped-ion system[32]. Moreover, different from the microwave cooling scheme[33], in which the magnetic tip with a fixed MFG is attached at the end of the cantilever, the cooling in our case is made by lasers, which ensure that the cooling rate (the cooling speed) in our scheme is larger (faster) than in the previous scheme[33], and the MFG in our idea is independent from the cantilever, but generated by the coils and controlled by the external electric current. The MFG in our design is evidently more flexibly adjustable.

More specifically, we show below that the addition of the Stark-shift gate makes the cooling more powerful than the optics-based EIT cooling in a previous scheme[29], and is particularly useful for the cantilever of lower vibrational frequency under weaker laser irradiation. This is much different from the strong coupling condition required in previous EIT-like schemes using cavities[35,36]. Since the cooling of the low-frequency cantilevers down to the ground state is still challenging with current technology, and the requirement of weak laser irradiation can reduce the experimental difficulty, our scheme is of practical application in exploring quantum properties of the nanomechanical cantilevers.

Results

The cooling of a NV-cantilever system by a Stark-shift gate. Our system is modeled as in Fig. 1(a), where a negatively charged NV center is attached at the end of a nanomechanical cantilever under a strong MFG. The ground state of the NV center is a spin triplet with a zero-field splitting $2\pi \times 2.87$ GHz between $m_s = 0$ and $m_s = \pm 1$, where m_s is the projection of the total electron spin $S = 1$ along the z-axis. The sublevels $m_s = \pm 1$ are employed for qubit encoding in our cooling scheme, with $m_s = -1$ as $|0\rangle$ and $m_s = +1$ as $|1\rangle$. According to the selection rule of the transitions[37,38], the state $|0\rangle$ ($|1\rangle$) may be coupled to the excited state $|A_2\rangle$ by a polarized laser[29,37–39]. $|A_2\rangle$ is an entangled state involving the components $|0\rangle$, $|1\rangle$ and the orbital states, and keeps separate enough from neighboring levels[38]. The state $|0\rangle$

can be coupled to $|1\rangle$ by an effective classical field due to two-photon Raman process (Adopted in the present work; see Methods for details) or by a stress applied perpendicularly to the axial direction of the NV center[40]. In Fig. 1(b), the σ_-^0 (σ_+^1) polarized laser owns the frequency ω_0 (ω_1) and the Rabi frequency Ω_0 (Ω_1). The effective classical field is with the frequency ω_L and the Rabi frequency Ω_L.

It should be noted that there are leakages from the excited state $|A_2\rangle$ down to the metastable state $|^1A_1\rangle$ (not shown in Fig. 1(b)), which would stop the cooling process. To solve this problem, we have to employ $m_s = 0$ and other auxiliary states to recycle the cooling process, as discussed in[29] but not reiterated in the present paper. Furthermore, different from the trapped-ion system, in which the coupling between the internal and the vibrational degrees of freedom is caused by the mechanical effect of light[41], our model employs the MFG to provide the coupling between the NV center and the vibration of the cantilever. The MFG consists of a coil wrapping a permanent magnet core, controlled by the external electric current.

The Hamiltonian of the system in units of $\hbar = 1$ is given by

$$\begin{aligned} H &= \omega_k a^\dagger a + \omega_A |A_2\rangle\langle A_2| + g_e\mu_B B(0)(|1\rangle\langle 1| - |0\rangle\langle 0|) \\ &\quad + \frac{\Omega}{2}(|A_2\rangle\langle 1|e^{-i\omega_1 t} + |A_2\rangle\langle 0|e^{-i\omega_0 t} + h.c.) + \frac{\Omega_L}{2}(|0\rangle\langle 1|e^{i\omega_L t} + h.c.) \\ &\quad + \lambda(|1\rangle\langle 1| - |0\rangle\langle 0|)(a^\dagger + a), \end{aligned} \tag{1}$$

where $a^\dagger$ (a) is the creation (annihilation) operator of the cantilever vibration with frequency ω_k, ω_A is regarding $|A_2\rangle$, $B(0)$ is the constant magnetic field strength, g_e is the g-factor and μ_B is the Bohr magneton. $\Omega(=\Omega_0=\Omega_1)$ and Ω_L are the Rabi frequencies regarding irradiation from the laser and the effective classical field. $\lambda = g_e\mu_B B'(0)x_0$ is the coupling due to the MFG $B'(0)$ with $x_0 = 1/\sqrt{2M\omega_k}$ and a cantilever mass M[33,34,42]. Although the NV center is sensitive to the strain, we suppose a low strain condition throughout this work, which ensures that the employed excited state $|A_2\rangle$ robustly owns stable symmetry properties[38].

To understand the cooling physical picture and simplify the calculation, we make a unitary transformation on equation (1). In the rotating frame, we have $|\psi^{\rm rot}(t)\rangle = e^{-iRt}|\psi(t)\rangle$ and $H^{\rm rot} = e^{-iRt}H(t)e^{iRt} + R$ with $R \equiv \omega_1|1\rangle\langle 1| + \omega_0|0\rangle\langle 0|$[43]. Under the near-resonance condition $\omega_L \approx \omega_0 - \omega_1$, equation (1) can be rewritten in a time-independent form as $H^{\rm rot} = H_0 + V$, with

$$H_0 = \omega_k a^\dagger a - \Delta|A_2\rangle\langle A_2| + \frac{\sqrt{2}}{2}\Omega(|A_2\rangle\langle b| + h.c.) + \frac{1}{2}\Omega_L(|b\rangle\langle b| - |d\rangle\langle d|), \tag{2}$$

and

$$V = \lambda(|b\rangle\langle d| + |d\rangle\langle b|)(a^\dagger + a), \tag{3}$$

where $|b\rangle = \frac{1}{\sqrt{2}}(|1\rangle + |0\rangle)$ and $|d\rangle = \frac{1}{\sqrt{2}}(|1\rangle - |0\rangle)$ are the corresponding bright and dark states, respectively, and the detunings satisfy $\Delta \equiv \Delta_0 = \Delta_1$ with $\Delta_0 = \omega_0 - \omega_A - g_e\mu_B B(0)$ and $\Delta_1 = \omega_1 - \omega_A + g_e\mu_B B(0)$. Moreover, the last term in equation (2) describes the energy difference between the bright and dark states caused by the effective classical field for the Stark shift, by which a Stark-shift gate will be performed below for the cooling of the cantilever vibration. Besides, the coupling between the cantilever and the NV center is created by a strong MFG, which makes the first-order red-sideband transition dominate in the cooling process based on quantum interference. With assistance of the effective classical field, the energy difference between the dark and bright states is equal to the frequency of the cantilever vibration. As a result, the phonon is dissipated by the coupling due to the MFG with the assistance of external fields.

The cooling mechanics based on the Stark-shift gate. The cooling in our scheme is based on the Stark-shift gate. According to refs 32,42,43, the Stark-shift gate in the total Hamiltonian $H_0 + V$ is described by

$$H_{ss} = \omega_k a^\dagger a + \frac{1}{2}\Omega_L(|b\rangle\langle b| - |d\rangle\langle d|) + V. \tag{4}$$

In the interaction picture, after the rotating wave approximation is applied, the Hamiltonian in (4) can be rewritten as

$$H_I = \lambda(|b\rangle\langle d|ae^{i\delta t} + |d\rangle\langle b|a^\dagger e^{-i\delta t}), \tag{5}$$

with $\delta = \Omega_L - \omega_k$. When our model is operated at the work point of the Stark-shift gate ($\Omega_L = \omega_k$), the above Hamiltonain reduces to

$$H_I = \lambda(|b\rangle\langle d|a + |d\rangle\langle b|a^\dagger), \tag{6}$$

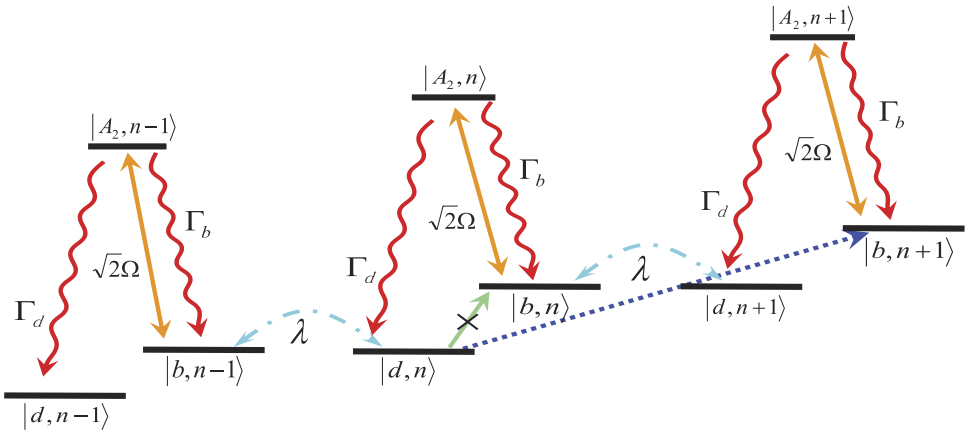

Figure 2. The schematic for the cooling mechanism. The Stark-shift-gate assisted cooling includes an effective classical field creating the Stark shift of the ground state, a strong MFG whose coupling λ leads to the red-sideband transition $|d, n\rangle \leftrightarrow |b, n-1\rangle$, and the optical lasers couple the bright state $|b\rangle$ to the excited state $|A_2\rangle$. The optical lasers should satisfy the two-phonon resonance condition ($\Delta_0 = \Delta_1$), which yields elimination of the carrier transition between $|d, n\rangle$ and $|b, n\rangle$ and suppression of the blue-sideband transition between $|d, n\rangle$ and $|b, n+1\rangle$. So the strong MFG only contributes to the red-sideband transition. In our treatment, we suppose $\Gamma_d = \Gamma_b = \Gamma/2$ and $\Gamma = \gamma_1 + \gamma_2$, and other parameters are defined in the text or in Fig. 1.

which is a typical Jaynes-Cummings interaction for the first-order red-sideband transition between the dark and bright states, leading to the phonon number change in the cantilever vibration.

The cooling process in our scheme is described in Fig. 2. In terms of equation (6), if the system is initially in the state $|d, n+1\rangle$, the only possible transition is from $|d, n+1\rangle$ to $|b, n\rangle$, which is caused by the Stark-shift gate. It results from the fact that the blue-sideband transition and the carrier transition relevant to the dark state $|d\rangle$ are suppressed by quantum interference. In the laboratory frame, the transition $|b, n\rangle \leftrightarrow |A_2, n\rangle$ is actually driven by two lasers with the same Rabi frequencies and detunings. As it is plotted in Fig. 2, the spin state is first excited to $|A_2, n\rangle$, and then decays to the bright state $|b, n\rangle$ or the dark state $|d, n\rangle$. If the decay is to the dark state $|d, n\rangle$, one phonon is lost from the cantilever vibration due to H_I and the cooling goes to the next step. But if the decay is to the bright state $|b, n\rangle$, the state will be pumped to the excited state $|A_2, n\rangle$ again, and this cycle of the laser cooling will be repeated until the decay is to the dark state.

A clearer picture for above cooling process with the phonon dissipation governed by the transition $|d, n+1\rangle \leftrightarrow |b, n\rangle$ can be found in Supplementary Information by numerically calculating the fluctuation spectra. We may find that the carrier transition $|d, n\rangle \rightarrow |b, n\rangle$ is totally suppressed by the destructive interference, and the blue-sideband transition $|d, n\rangle \rightarrow |b, n+1\rangle$ is largely suppressed. As a result, repeating the laser cooling cycles, we will finally cool the cantilever down to the vibration ground state.

Before going further to the numerical calculation, we simply compare the Stark-shift-gate cooling with the EIT cooling in ref. 29. From the schematic illustrations, both of them share the similar quantum interference process and steady state, which can effectively suppress the blue-sideband transition and the carrier transition. Besides, the Stark-shift-gate cooling goes beyond the EIT cooling by an additional coupling, which drives the transition between the dark and bright states, constituting a Jaynes-Cummings interaction by the first-order red-sideband transition at the work point $\Omega_L = \omega_k$. As a result, different from the EIT cooling, the Stark-shift-gate cooling works with the efficiency independent from the cooling laser strength, but mainly relevant to the work point.

The analytical and numerical treatments for the cooling. By utilizing the perturbation theory and the non-equilibrium fluctuation-dissipation relation, the Hamiltonian H^{rot} (equation (2) plus equation (3)) yields the heating (cooling) coefficient A_+ (A_-) caused by the external fields as below,

$$A_{\pm} = \frac{2\Gamma\lambda^2\Omega^2}{[\Omega^2 + (\mp\omega_k - \Omega_L)(\pm 2\omega_k - 2\Delta + \Omega_L)]^2 + \Gamma^2(\mp\omega_k - \Omega_L)^2}, \quad (7)$$

whose deduction in details can be found in Methods and Supplementary Information. Γ is the total decay rate regarding $|A_2\rangle$. The heating (cooling) coefficient in equation (7) is different from the one obtained previously[26,29,30,44], but can be reduced to the result in[32] when $\Omega_L = \omega_k$. This is due to the fact that both[32] and our scheme share the same work point for the Stark-shift gate, related to the Rabi

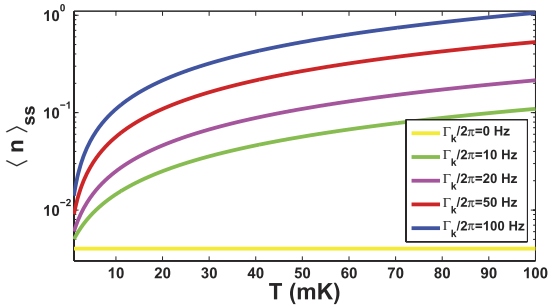

Figure 3. The final phonon number $\langle n \rangle_{ss}$ (in logarithmic scale) versus the environmental temperature T and the vibrational decay rate Γ_k, where we have taken the parameter values $\omega_k/2\pi = 2$ MHz, $\Omega/2\pi = 2$ MHz, $\Omega_L = \omega_k$ and $\Delta = 0$[37], as well as $\Gamma/2\pi = 15$ MHz and $\lambda/2\pi = 0.115$ MHz[33,34,50].

frequency of the effective classical field and the vibrational frequency of the ion or cantilever. Nevertheless, the cooling (heating) efficiency in[32] only depends on the Rabi frequency of the microwave field, but ours is relevant to the effective classical field Rabi frequency assisted by the MFG coupling λ.

A proper analysis of the phonon dissipation must consider the non-zero temperature environmental noise, since compared to the trapped-ion system the cantilever with much larger volume and mass is more sensitive to the environment. Using the techniques developed previously[26,29], we obtain following analytical expression of the time-dependent average phonon number,

$$\langle n(t) \rangle = \langle n \rangle_{ss} + e^{-(W+\Gamma_k)t} \left[\langle n(0) \rangle - \langle n \rangle_{ss} \right], \tag{8}$$

where the cooling rate $W = A_- - A_+$ originates from the interaction between the NV center and the external fields[30,44]. The final average phonon number is

$$\langle n \rangle_{ss} = [A_+ + K(\omega_k)\Gamma_k]/(W + \Gamma_k), \tag{9}$$

where $\Gamma_k \equiv \omega_k/q$ is the vibrational decay rate with the quality factor q of the cantilever, and $K(\omega_k) = 1/(e^{\hbar\omega_k/k_B T} - 1)$ is the thermal occupation for the cantilever vibrational degrees of freedom[26] with the Boltzmann constant k_B and the environmental temperature T, respectively. As plotted in Fig. 3, our scheme works even for the NR with a low frequency (e.g., $\omega_k/2\pi = 2$ MHz). Compared with the previous scheme[29], our scheme can achieve a good cooling under very weak cooling laser radiation ($\Omega/2\pi = 2$ MHz). With the same environmental temperature T, our scheme works for a smaller decay rate Γ_k. More specific discussion on this point can be found later.

For a deeper understanding of our cooling scheme, we may focus on the work point $\Omega_L = \omega_k$ of the Stark-shift gate, which simplifies the heating and cooling coefficients in equation (7) to be

$$A_+ = \frac{2\Gamma\lambda^2\Omega^2}{4\Gamma^2\omega_k^2 + (\Omega^2 - 6\omega_k^2 + 4\Delta\omega_k)^2}, \qquad A_- = \frac{2\Gamma\lambda^2}{\Omega^2}. \tag{10}$$

As plotted in Fig. 4(Left), A_+ (A_-) increases (decreases) with Ω. To make sure an efficient cooling, we should have A_- to be larger than A_+, implying an upper limit $\Omega^2 \leq M_2 = \omega_k^2(\Gamma^2 + 4\Delta^2 + 9\omega_k^2 - 12\Delta\omega_k)/(3\omega_k^2 - 2\Delta\omega_k)$ from the above analytical expressions. Moreover, both the left and right panels of Fig. 4 show that the faster cooling and the minimal final phonon number prefer smaller laser Rabi frequency. The extreme case happens at $\Omega = 0$, in which we have $W = A_-$ due to negligible A_+, and thereby $\langle n \rangle_{ss}$ tends to minimum. However, this is a non-physical condition since $\Omega = 0$ means no laser irradiation. In our case, if the cooling works, $\Omega^2 > M_1 = \max[\Gamma\lambda, \omega_k\lambda, \Delta\lambda]$ (meaning the internal dynamics faster than the external dynamics, e.g., $\sqrt{M_1}/2\pi = 1.3$ MHz in Fig. 4) should be satisfied. As such, we reach a trade-off regime for the laser irradiation $M_1 < \Omega^2 \leq M_2$. On the other hand, the laser detuning Δ involved in A_+ also has influence on the cooling. To have a larger cooling rate, a larger blue detuning (i.e., $\Delta > 0$) is required for the condition $\Omega^2 - 6\omega_k^2 > 0$, while a larger red detuning ($\Delta < 0$) is necessary when $\Omega^2 - 6\omega_k^2 \leq 0$ is satisfied.

The analytical results above (i.e., equations (7) and (10)) are obtained under the perturbation and the adiabatic condition. This implies that the real cooling effect should be justified by the small values of Ω, for which the adiabatic condition is not fully satisfied. To this end, we have numerically calculated the cooling rate W with respect to Ω at the work point of the Stark-shift gate. We may find from Fig. 5 that the discrepancy between the analytical and numerical results appears within the regime $\Omega/2\pi < 3$ MHz where the adiabatic condition is no longer valid. If we check this regime more carefully, we find that the discrepancy is bigger for the lower frequency of the cantilever, which is due to the fact that the lower

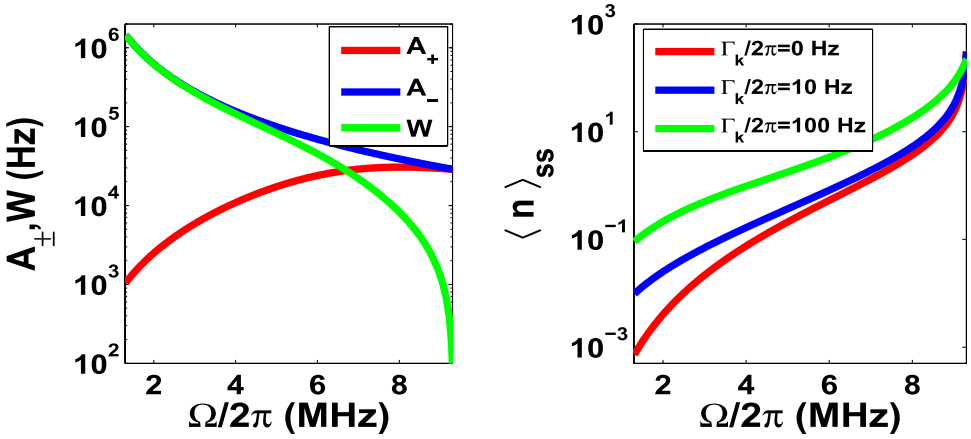

Figure 4. (Left) The heating coefficient A_+, the cooling coefficient A_-, and the cooling rate $W=A_- - A_+$ (in logarithmic scale) versus $\Omega/2\pi$. (Right) The final average phonon number $\langle n\rangle_{ss}$ (in logarithmic scale) versus $\Omega/2\pi$ for different Γ_k, where we consider $\Omega_L=\omega_k$ and the other parameters take the values as $\omega_k/2\pi=2$ MHz, $\Gamma/2\pi=15$ MHz, $T=20$ mK, $\lambda/2\pi=0.115$ MHz and $\Delta=0$.

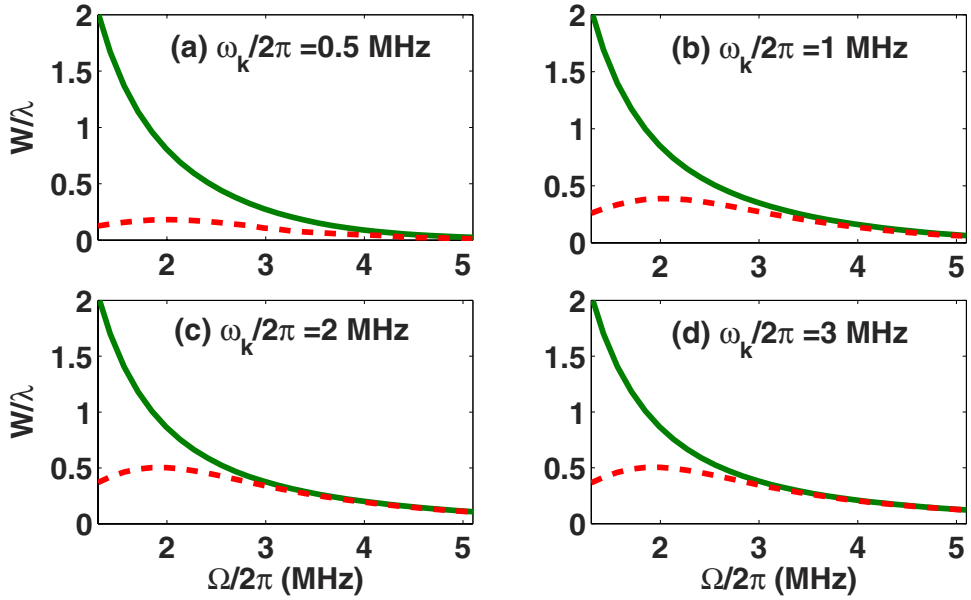

Figure 5. The cooling rate W/λ versus the Rabi frequency $\Omega/2\pi$ where the work point $\Omega_L=\omega_k$ is satisfied. The parameters take values as $\lambda/2\pi=0.115$ MHz, $\Gamma/2\pi=15$ MHz and $\Delta=0$. The solid curves are the analytical results of the cooling rate W by equation (10) and the dashed curves are plotted by solving the master equations of H^{rot}.

frequency cantilever owning a larger λ (λ is a function inversely proportional to $\sqrt{\omega_k}$) makes the rotating wave approximation less valid in obtaining the work point of the Stark-shift gate.

The physical reason for the cooling rates plotted in Fig. 5 can be understood by the decay and the pumping in the cooling process. Since the transition between the bright and dark states is dipolar forbidden, we excite the system from the bright state $|b\rangle$ to the excited state $|A_2\rangle$, and then it decays down to the dark state $|d\rangle$. With a stronger pump light, the effective decay from the bright state to the dark state would be bigger, which yields a larger cooling rate. However, a much stronger light would shift the bright state and thereby weaken the red-sideband transition. As a result, with increasing Ω, the cooling rate increases at first, and then decreases, as examined by numerics in Fig. 5. However, the analytical solutions in equation (10) could not exactly describe the above cooling process if $\Omega/2\pi<3$ MHz.

Both the analytical and numerical results imply that our cooling scheme is more powerful than previously proposed ones[25–29], particularly in the case of the lower vibrational frequency ($\omega_k/2\pi<1$ MHz) and the weaker laser field ($\Omega/2\pi<3$ MHz). Considering the numerical results in Figs 5 and 6, we observe

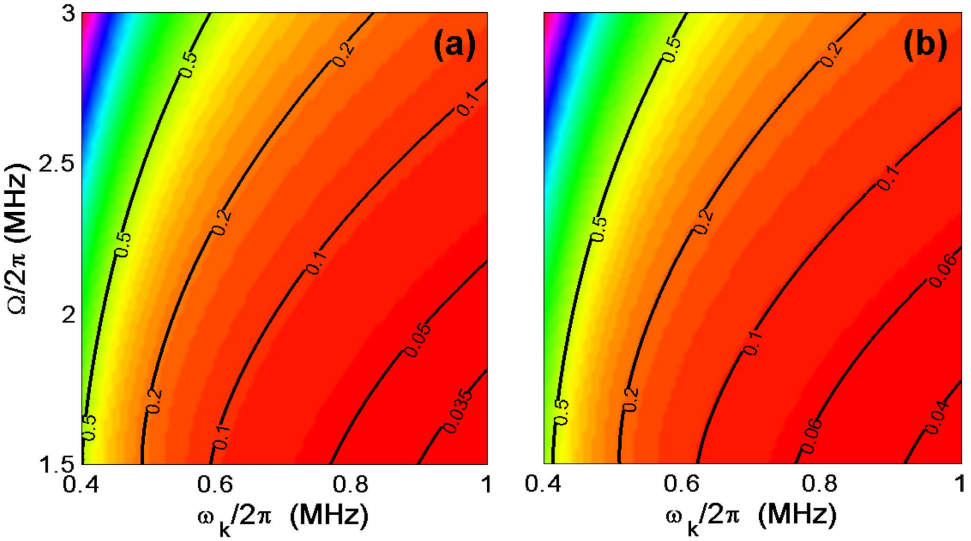

Figure 6. The final average phonon number $\langle n\rangle_{ss}$ versus the vibrational frequency $\omega_k/2\pi$ and Rabi frequency $\Omega/2\pi$, where the work point $\Omega_L=\omega_k$ is satisfied. (**a**) The case of zero temperature environment without considering the vibrational decay. (**b**) The case of the environmental temperature $T=20\,\mathrm{mK}$ with the vibrational decay rate $\Gamma_k/2\pi=1\,\mathrm{Hz}$. Other parameters employed are $\lambda/2\pi=0.115\,\mathrm{MHz}$, $\Gamma/2\pi=15\,\mathrm{MHz}$ and $\Delta=0$.

that the maximal cooling rate W_{max} in our case can be more than 0.5λ once $\omega_k/2\pi\geq 2\,\mathrm{MHz}$, implying a much better cooling than in the resolved sideband regime in the laboratory representation[33]. Moreover, compared with[29], our scheme reaches the maximal cooling rate $W_{max}>0.5\lambda$ by a weaker cooling laser, e.g., approximately $\Omega/2\pi=2\,\mathrm{MHz}$, for the lower frequency vibrational mode, e.g., $\omega_k/2\pi=2\,\mathrm{MHz}$. In contrast, reaching such a cooling rate W in[29] requires $\omega_k/2\pi=10\,\mathrm{MHz}$ and $\Omega/2\pi=80\,\mathrm{MHz}$, where the Rabi frequency Ω is linearly proportional to the vibrational frequency ω_k. So our scheme can release the demanding experimental requirement of strong laser beams compared with the previous scheme. In addition, the figures also present that cooling the cantilever with $\omega_k/2\pi<1\,\mathrm{MHz}$ is less efficient compared with $\omega_k/2\pi=2$ or 3 MHz, but still working. For example, from Figs 5 and 6, we know that our scheme can cool the cantilever down to $\langle n\rangle_{ss}\approx 0.2$ with the cooling rate $W_{max}\simeq 0.1816\lambda$ in the case of $\omega_k/2\pi=0.5\,\mathrm{MHz}$ and $\Omega/2\pi=2\,\mathrm{MHz}$. In contrast, the schemes in[29,33] can work only in the case of $\omega_k/2\pi\geq 1\,\mathrm{MHz}$ and a larger Rabi frequency (e.g., $\Omega/2\pi=5\,\mathrm{MHz}$[29]).

Discussion

In terms of the experimental parameters reported[34,45,46], we may choose following parameter values for our scheme. The NR with a frequency $\omega_k\simeq 2\pi\times 2\,\mathrm{MHz}$ takes a decay rate $\gamma=100\,\mathrm{Hz}$. The laser with wavelength $\lambda_{laser}\equiv 2\pi c/\omega_{0,1}\simeq 637$ nm and power $P\ll 100\,\mu W$ can induce the Rabi frequency $\Omega=2\pi\times 2\,\mathrm{MHz}$. Then, under the action of the external MFG ($\sim 10^7\,\mathrm{T/m}$[33,46]), the NR can be cooled down to its ground state with a mean phonon number $\langle n\rangle_{ss}<0.1$ and a NV-cantilever coupling $\lambda\simeq 2\pi\times 0.115$ MHz at the temperature $T=20\,\mathrm{mK}$.

To check how well our scheme works in a realistic system, we consider below the variation of the cooling effect with respect to the deviation from the work point $\Omega_L=\omega_k$ of the Stark-shift gate. Figure 7 presents that the average phonon number $\langle n\rangle_{ss}$ changes slightly with ω_k, but this change becomes less evident for a larger ω_k. Since the work point only maximizes A_-, the fact that $\langle n\rangle_{ss}$ is determined by both A_- and A_+ leads to the onset of the minimal average phonon number deviated from the work point. For a given decay rate Γ_k, the larger ω_k is more beneficial for cooling at the work point, and less sensitive to the deviation from the work point. In summary, our proposed cooling is robust against the experimental imperfection.

We should also assess the influence from the nuclear spin bath in the NV center, which might seriously affect the final average phonon number $\langle n\rangle_{ss}$ and the cooling time t. To this end, we have considered some concrete values of the parameters, such as $\langle n\rangle_{initial}=5$, $\omega_k/2\pi=2\,\mathrm{MHz}$, $\lambda/2\pi=0.115\,\mathrm{MHz}$, $\Gamma/2\pi=15\,\mathrm{MHz}$, $T=20\,\mathrm{mK}$, $\Omega/2\pi=2\,\mathrm{MHz}$, $\Omega_L=\omega_k$, $\Delta=0$ and $\Gamma_k/2\pi=10\,\mathrm{Hz}$. Provided the nuclear spin bath taking the random energy $\delta_n/2\pi\leq 0.1\,\mathrm{MHz}$ (0.5 MHz), the final average phonon number increases from $\langle n\rangle_{ss}=0.0399$ to 0.0436 (0.1729) and the corresponding cooling takes time from $t=39.7\,\mu s$ to $42.2\,\mu s$ ($97.5\,\mu s$). Therefore, suppressing the influence from the nuclear spin bath is very important in order to achieve our cooling scheme. Possible approaches include the dynamic nuclear polarization

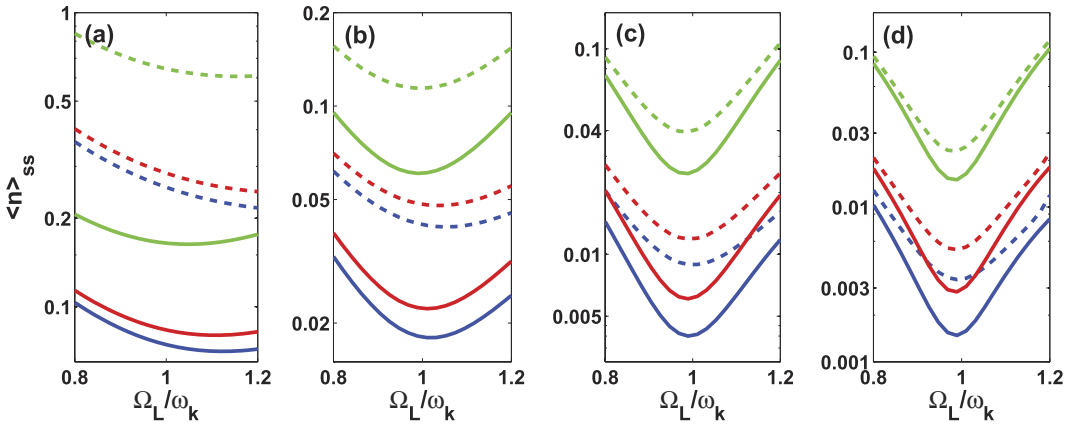

Figure 7. The final average phonon number $\langle n\rangle_{ss}$ (in logarithmic scale) versus Ω_L/ω_k for different ω_k, where (**a**) $\omega_k/2\pi = 0.5$ MHz; (**b**) $\omega_k/2\pi = 1$ MHz; (**c**) $\omega_k/2\pi = 2$ MHz; (**d**) $\omega_k/2\pi = 3$ MHz. In every panel, the solid curves are simulated by equation (9) and the dash curves are the numerical results by the master equation of H^{rot}. The pairs of the curves, from the bottom to top, correspond to $\Gamma_k/2\pi = 0$, 1 and 10 Hz, respectively. Other parameters take the values as $\Omega/2\pi = 2$ MHz, $\Gamma/2\pi = 15$ MHz, $T = 20$ mK, $\lambda/2\pi = 0.115$ MHz and $\Delta = 0$.

technology[47] and the isotopic purification of NV center[48], which have been widely adopted in the field of spintronics.

In summary, we have studied an efficient cooling of the cantilever vibration by a dynamic Stark-shift gate, in which the carrier transition and the blue-sideband transition can be effectively suppressed when the operation is made around the work point of the Stark-shift gate. We have shown the possibility to cool the low-frequency cantilever down to the vicinity of the ground state using weak cooling lasers. Most of the parameter values are taken from experimental reports. Particularly, our scheme is less stringent experimentally compared to previous schemes, such as with weak laser radiation (i.e., smaller laser power), working for lower-frequency cantilevers (i.e., usually employed cantilevers) and with a feasible MFG ~10^7 T/m[33,46] (without special requirement for the magnetic field strength). As such our scheme is experimentally relevant and feasible.

Compared to the previous proposal for the trapped ion[32], our scheme has major differences at following two points. The essential difference is the much larger mass of the cantilever compared to the trapped ion. As a result, in our case the coupling of the motional degrees of freedom of the cantilever to the spin degrees of freedom of the NV center is provided by a strong magnetic field gradient. In contrast, a laser radiation simply achieves this coupling[32]. The second difference lies in different technical requirements. For example, the effective coupling strength Ω_L is achieved by using a Raman transition in our case. In a word, the dynamical Stark-shift in our case is from the classical-field-assisted MFG, rather than the laser field as in[32].

Finally, we have to mention that the analytical results we obtained, although not always accurate, have presented a clear relationship of the final average phonon number with the vibrational decay rate and the bath temperature. Moreover, we have also analyzed the limitation of the maximal cooling rate. We argue that our scheme is experimentally timely and would be useful for achieving an efficient cooling of the cantilever vibration using currently available techniques.

Methods

Two-photon Raman process. The ground state sublevels $|0\rangle$ and $|1\rangle$ cannot be coupled directly unless the external magnetic field applied is not exactly in parallel with the NV crystal axis. Unfortunately, our model requires the external magnetic field to be applied exactly along the axis of the NV crystal. To solve this problem, we consider an effective coupling between $|0\rangle$ and $|1\rangle$ created by a two-photon Raman process, where two additional lasers with large detunings from the $|A_2\rangle$ are employed to couple, respectively, $|0\rangle$ ($|1\rangle$) to the exited state $|A_2\rangle$ with frequency ω_0' (ω_1') and Rabi frequency Ω_0' (Ω_1'). Under the large detuning Δ' ($|\Delta'| \gg |\Delta|, |\overline{\Delta}|$) where $\Delta' = \omega_1 - \omega_1' = \omega_0 - \omega_0'$, the additional lasers can induce an effective coupling between $|0\rangle$ and $|1\rangle$ with the coupling intensity $\Omega_{\text{eff}} = -\frac{\Omega'^2}{4\Delta'}$. Therefore, the two-photon Raman process can realize the effect of an effective classical field with $\Omega_L = \Omega_{\text{eff}}$. (See Supplementary Information for details).

The cooling and heating rates. In what follows, we derive the cooling and heating rates by the non-equilibrium fluctuation-dissipation relation. Using $X = x_0(a^\dagger + a)$, we rewrite the interaction

Hamiltonian in equation (3) as $V = \frac{\lambda}{x_0} X (|b\rangle\langle d| + |d\rangle\langle b|)$. As a result, the Heisenberg operator $F(t)$ is given by $F(t) = -\frac{d}{dX} V \Big|_{X=0} = -\frac{\lambda}{x_0}\sigma_x^{bd}$ where we have defined $\sigma_x^{m,n} = |m\rangle\langle n| + |n\rangle\langle m|$ with $m, n = A_2$, b, d. The steady state ρ_{ss} for the NV center can be solved as $\rho_{ss} = |d\rangle\langle d|$ by the Bloch equations of H^{rot} [49] (see Supplementary Information). When the NV center is in the dark state, the fluctuation spectrum is written as

$$\begin{aligned} S(\omega) &= \eta^2\omega^2 \int_0^\infty \mathrm{d}t e^{i\omega t} \langle \sigma_x^{bd}(t)\sigma_x^{bd}(0)\rangle_{ss} \\ &= \frac{\eta^2\omega^2[\Gamma + i(\Omega_L - 2\omega - 2\Delta]}{-2\nu^2 - 2\omega\Delta + \Omega^2 + 3\omega\Omega_L + 2\Delta\Omega_L - \Omega_L^2 + i\Gamma(\Omega_L - \omega)}. \end{aligned} \tag{11}$$

The corresponding heating (cooling) coefficient can be obtained by $A_\pm = 2\,\mathrm{Re}\{S(\mp\omega_k)\}$.

The numerical simulation. To check the analytical results, we simulate the dynamical process by the master equation of the density matrix ρ. The master equation for the density matrix ρ in the Lindblad form[26,29] is given by

$$\begin{aligned} \frac{d}{dt}\rho &= -i[H^{\mathrm{rot}}, \rho] + [K(\omega_k) + 1]\mathscr{D}(\Gamma_k, a) + K(\omega_k)\mathscr{D}(\Gamma_k, a^\dagger) \\ &\quad + \mathscr{D}(\Gamma_b, |b\rangle\langle A_2|) + \mathscr{D}(\Gamma_d, |d\rangle\langle A_2|), \end{aligned} \tag{12}$$

where $\mathscr{D}(\gamma, A)\rho = \frac{\gamma}{2}(A\rho A^\dagger - \rho A^\dagger A - A^\dagger A\rho)$, $\Gamma_k = \omega_k/q$ and $K(\omega_k) = [e^{\hbar\omega_k/k_B T} - 1]^{-1}$ with the cantilever quality q and the environmental temperature T.

References

1. Weis, S. *et al.* Optomechanically induced transparency. *Science* **330,** 1520–1523 (2010).
2. Nunnenkamp, A., Borkje, K. & Girvin, S. M. Single-Photon Optomechanics. *Phys. Rev. Lett.* **107,** 063602 (2011).
3. Rabl, P. Photon blockade effect in optomechanical systems. *Phys. Rev. Lett.* **107,** 063601 (2011).
4. Imoto, N., Haus, H. A. & Yamamoto, Y. Quantum nondemolition measurement of the photon number via the optical Kerr effect. *Phys. Rev. A* **32,** 2287 (1985).
5. Braginsky, V. B. & Manukin, A. B. *Measurements of weak forces in physics experiments* edited by Douglass, D. H. (Chicago University Press, Chicago, 1977).
6. Chotorlishvili, L. *et al.* Entanglement between nitrogen vacancy spins in diamond controlled by a nanomechanical resonator. *Phys. Rev. B* **88,** 085201 (2013).
7. Irish, E. K. & Schwab, K. Quantum measurement of a coupled nanomechanical resonator–Cooper-pair box system. *Phys. Rev. B* **68,** 155311 (2003).
8. LaHaye, M. D., Suh, J., Echternach, P. M., Schwab, K. C. & Roukes, M. L. Nanomechanical measurements of a superconducting qubit. *Nature* **459,** 960–964 (2009).
9. Ndieyira, J. W. *et al.* Nanomechanical detection of antibiotic–mucopeptide binding in a model for superbug drug resistance. *Nat. Nanotech.* **11** 691–696 (2008).
10. Tetard, L. *et al.* Imaging nanoparticles in cells by nanomechanical holography. *Nat. Nanotech.* **8,** 501 (2008).
11. Treutlein, P. *et al.* Bose-Einstein condensate coupled to a nanomechanical resonator on an atom chip. *Phys. Rev. Lett.* **99,** 140403 (2007).
12. Wilson-Rae, I., Zoller, P. & Imamoglu, A. Laser cooling of a nanomechanical resonator mode to its quantum ground state. *Phys. Rev. Lett.* **92,** 075507 (2004).
13. Teufel, J. D. *et al.* Sideband cooling of micromechanical motion to the quantum ground state. *Nature* **475,** 359–363 (2011).
14. Li, Y., Wang, Y. D., Xue, F. & Bruder, C. Cooling a micromechanical beam by coupling it to a transmission line. *Phys. Rev. B* **78,** 134301 (2008).
15. Yoshie, T. *et al.* Vacuum Rabi splitting with a single quantum dot in a photonic crystal nanocavity. *Nature* **432,** 200–203 (2004).
16. Wilson-Rae, I., Nooshi, N., Zwerger, W. & Kippenberg, T. J. Theory of ground state cooling of a mechanical oscillator using dynamical backaction. *Phys. Rev. Lett.* **99,** 093901 (2007).
17. Marquardt, F., Chen, J. P., Clerk, A. A. & Girvin, S. M. Quantum theory of cavity-assisted sideband cooling of mechanical motion. *Phys. Rev. Lett.* **99,** 093902 (2007).
18. Xue, F., Wang, Y. D., Liu, Y. X. & Nori, F. Cooling a micromechanical beam by coupling it to a transmission line. *Phys. Rev. B* **76,** 205302 (2007).
19. Naik, A. *et al.* Cooling a nanomechanical resonator with quantum back-action. *Nature* **443,** 193–196 (2006).
20. Mari, A. & Eisert, J. Cooling by heating: very hot thermal light can significantly cool quantum systems. *Phys. Rev. Lett.* **108,** 120602 (2012).
21. Zhang, J. Q., Li, Y. & Feng, M. Cooling a charged mechanical resonator with time-dependent bias gate voltages. *J. Phys.: Condens. Matter* **25,** 142201 (2013).
22. Li, Y., Wu, L. A. & Wang, Z. D. Fast ground-state cooling of mechanical resonators with time-dependent optical cavities. *Phys. Rev. A* **83,** 043804 (2011).
23. Deng, Z. J., Li, Y., Gao, M. & Wu, C. W. Performance of a cooling method by quadratic coupling at high temperatures. *Phys. Rev. A* **85,** 025804 (2012).
24. Li, Y, Wu, L. A., Wang, Y. D. & Yang, L. P. Nondeterministic ultrafast ground-state cooling of a mechanical resonator. *Phys. Rev. B* **84,** 094502 (2011).
25. Li, Z. Z., Ouyang, S. H., Lam, C. H. & You, J. Q. Cooling a nanomechanical resonator by a triple quantum dot. *Europhys. Lett.* **95,** 40003 (2011).
26. Xia, K. Y. & Evers, J. Ground state cooling of a nanomechanical resonator in the nonresolved regime via quantum interference. *Phys. Rev. Lett.* **103** 227203 (2009).

27. Zhu, J. P., Li, G. X. & Ficek, Z. Two-particle dark-state cooling of a nanomechanical resonator. *Phys. Rev. A* **85** 033835 (2012).
28. Zhu, J. P. & Li, G. X. Ground-state cooling of a nanomechanical. *Phys. Rev. A* **86** 053828 (2012).
29. Zhang, J. Q. *et al.* Fast optical cooling of nanomechanical cantilever with the dynamical Zeeman effect. *Optics Express* **21,** 029695 (2013).
30. Morigi, G., Eschner, J. & Keitel C. H. Ground state laser cooling using electromagnetically induced transparency. *Phys. Rev. Lett.* **85** 4458 (2000).
31. Roos, C. F. *et al.* Experimental demonstration of ground state laser cooling with electromagnetically induced transparency. *Phys. Rev. Lett.* **85,** 5547 (2000).
32. Retzker, A. & Plenio, M. B. Fast cooling of trapped ions using the dynamical Stark shift. *New J. Phys.* **9,** 279 (2007).
33. Rabl, P. *et al.* Strong magnetic coupling between an electronic spin qubit and a mechanical resonator. *Phys. Rev. B* **79,** 041302 (2009).
34. Arcizet, O. *et al.* A single nitrogen-vacancy defect coupled to a nanomechanical oscillator. *Nat. Phys.* **7,** 879–883 (2011).
35. Genes, C., Ritsch, H., Drewsen, M. & Dantan, A. Atom-membrane cooling and entanglement using cavity electromagnetically induced transparency. *Phys. Rev. A* **84,** 051801 (2011).
36. Zhang, S. *et al.* Ground state cooling of an optomechanical resonator assisted by a λ-type atom. *Opt. Exp.* **22,** 028118–028131 (2014).
37. Maze, J. R. *et al.* Properties of nitrogen-vacancy centers in diamond: the group theoretic approach. *New J. Phys.* **13,** 025025 (2011).
38. Togan, E. *et al.* Quantum entanglement between an optical photon and a solid-state spin qubit. *Nature* **466,** 730–734 (2010).
39. Chen, Q., Yang, W. L., Feng, M. & Du, J. F. Entangling separate nitrogen-vacancy centers in a scalable fashion via coupling to microtoroidal resonators. *Phys. Rev. A* **83,** 054305 (2011).
40. MacQuarrie, E. R., Gosavi, T. A., Jungwirth, N. R., Bhave, S. A. & Fuchs, G. D. Mechanical spin control of nitrogen-vacancy centers in diamond. *Phys. Rev. Lett.* **111,** 227602 (2013).
41. Morigi, G. & Eschner, J. Is an ion string laser-cooled like a single ion? *J. Phys. B: At. Mol. Opt. Phys.* **36,** 1041 (2003).
42. Mintert, F. & Wunderlich, C. Ion-trap quantum logic using long-wavelength radiation. *Phys. Rev. Lett.* **87,** 257904 (2001).
43. Gardiner, S. A. *Quantum measurement, quantum chaos, and Bose-Einstein condensates* dissertation (Leopold-Franzens-Universitat Innsbruck, 1977).
44. Morigi, G. Cooling atomic motion with quantum interference. *Phys. Rev. A* **67,** 033402 (2003).
45. Gröblacher, S., Hammerer, K., Vanner, M. R. & Aspelmeyer, M. Observation of strong coupling between a micromechanical resonator and an optical cavity field. *Nature* **460,** 724–727 (2009).
46. Kolkowitz, S. *et al.* Coherent sensing of a mechanical resonator with a single-spin qubit. *Science* **335,** 1603–1606 (2012).
47. Jacques, V. *et al.* J. Dynamic polarization of single nuclear spins by optical pumping of nitrogen-vacancy color centers in diamond at room temperature. *Phys. Rev. Lett.* **102,** 057403 (2009).
48. Ishikawa, T. *et al.* Optical and spin coherence properties of nitrogen-vacancy centers placed in a 100 nm thick isotopically purified diamond layer. *Nano Lett.* **12,** 2083–87 (2012).
49. Cirac, J. I., Blatt, R. & Zoller, P. Laser cooling of trapped ions in a standing wave. *Phys. Rev. A* **46,** 2668 (1992).
50. Rabl, P., Steixner, V. & Zoller, P. Quantum-limited velocity readout and quantum feedback cooling of a trapped ion via electromagnetically induced transparency. *Phys. Rev. A.* **72,** 043823 (2005).

Acknowledgements

JQZ thanks Xing Xiao, and Nan Zhao for helpful discussions. This work is supported by National Fundamental Research Program of China (Grants No. 2012CB922102 and No. 2013CB921803), National Natural Science Foundation of China (Grants No. 11274352 and No. 11304366) and the China Postdoctoral Science Foundation (Grants No. 2013M531771 and and No. 2014T70760).

Author Contributions

L.L.Y. contributed to numerical and prepared the first version of the manuscript, J.Q.Z. and S.Z. designed this work, J.Q.Z. and M.F. gave physical analysis. L.L.Y., J.Q.Z. and M.F. wrote the manuscript.

Additional Information

Supplementary information accompanies this paper at http://www.nature.com/srep

Competing financial interests: The authors declare no competing financial interests.

How to cite this article: Yan, L. *et al.* Fast optical cooling of a nanomechanical cantilever by a dynamical Stark-shift gate. *Sci. Rep.* **5**, 14977; doi: 10.1038/srep14977 (2015).